

Green Superhydrophobic Paper with Self-cleaning Properties Prepared via One-step Impregnation

Xiangbin Zhang¹, Shanshan Gao^{1,3,*}, Xiaoming Song^{1,2,4,*}, Jiale Wang¹, Xunqian Wu¹, Fushan Chen¹, Shiyuan Xie⁵

1. *Qingdao University of Science and Technology, Qingdao, Shandong Province, 266042, China*

2. *State Key Laboratory of Biobased Material and Green Papermaking, Qilu University of Technology (Shandong Academy of Sciences), Ji'nan, Shandong Province, 250353, China*

3. *Guangxi Key Laboratory of Clean Pulp & Papermaking and Pollution Control, Nanning, Guangxi Zhuang Autonomous Region, 530004, China*

4. *Kejian Kekang (Qingdao) Group Co., Ltd., Qingdao, Shandong Province, 266400, China*

5. *Linshu County Huaxing Paper Co., Linyi, Shandong Province, 276700, China*

Abstract: In this study, a green and pollution-free multifunctional superhydrophobic paper-based material was prepared using a simple and efficient dipping method. The superhydrophobic paper with a water contact angle (WCA) of 160° was prepared by attaching micro- and nanocomposite particles, made of stearic acid-modified chitosan and two kinds of titanium dioxide (TiO₂) nanoparticles of different sizes, to a paper substrate. The surface morphology, elemental composition, and wetting properties of the coatings were examined using scanning electron microscopy (SEM), X-ray photoelectron spectroscopy (XPS), Fourier transform infrared spectroscopy (FT-IR), and contact angle measurements. Additionally, superhydrophobic coatings exhibited good self-cleaning properties, liquid repellency, ease of repair, and antifouling properties in organic solutions.

Keywords: superhydrophobic; impregnation; green; paper-based; self-cleaning

Received: 27 March 2023; accepted: 12 September 2023; DOI: 10.26599/PBM.2023.9260021

1 Introduction

Based on bionic studies of the superhydrophobic properties of plants and animals in



Xiangbin Zhang, master candidate;

E-mail: zxb0720@126.com



*Corresponding author:

Xiaoming Song, professor; research interest: comprehensive utilization of biomass, biomass-based functional materials;

E-mail: xiaomingsong4007@163.com

nature, superhydrophobic properties can be successfully imparted to various substrates using various engineering techniques^[1-2], thus solving practical problems related to surface self-cleaning, friction and drag reduction, and the prevention of road ice formation^[3-4]. Water droplets glide effortlessly across the surface of lotus leaves, carrying away dirt and debris. This unique phenomenon has attracted the attention of scientists^[5-6]. Delving into microscopic examinations, Barthlott et al^[7] identified that this effect is a result of the combination of microscopic papillae and hydrophobic waxes on the leaf's surface. Feng et al^[8] further expanded on this research, discovering that the microscopic papillae on the lotus leaves possess even finer nanostructures. This intricate blend of micro- and nano-roughness imparts the superhydrophobic properties to lotus leaves.

Paper has a wide range of applications in industrial and agricultural production and everyday life^[9]. Paper is a green and nonpolluting material found everywhere in daily life and is widely used in agricultural and industrial production^[10]. Paper mainly consists of netted plant fibers that are abundant and inexpensive in nature^[11]. Moreover, plant fibers are nonpolluting, biodegradable, recyclable, and mechanically strong. Therefore, it is considered an attractive material. However, given that paper-based materials are susceptible to moisture, the paper performance decreases when water is absorbed, which limits its application^[12-13].

The emergence of superhydrophobic paper has provided an effective solution to this challenge, as it can dramatically improve the paper's resistance to moisture and water while also providing excellent self-cleaning and stain resistance properties^[14]. A prerequisite for fabricating superhydrophobic materials that are widely used in real-life application is a simple, efficient, and green preparation method^[4, 9].

Currently, the methods of preparing superhydrophobic paper include chemical grafting modification^[15-16], layer-by-layer self-assembly^[17-18], supercritical solution rapid expansion^[19], plasma treatment^[20-21], phase separation^[22-23], impregnation^[24-25], electrostatic spinning^[26-27], chemical vapor deposition^[28], and spraying^[29-30]. Impreg-

nation is equivalent to immersion in a solution. During the preparation process, the substrates must be immersed in the solution, and then the substances in the solvent can be attached to the paper surface via curing to obtain special properties^[31]. The paper prepared using this method exhibited good superhydrophobicity. The dip-coating technique was chosen because it is simple, widely applied, and provides a uniform coating.

Commonly used materials for the construction of micro/nano rough structure include nano titanium dioxide (TiO_2)^[32-33], SiO_2 ^[34-35], Al_2O_3 ^[36-37], mixed wax^[38], and zirconia^[39-40]. Considering the cost, preparation process, and other factors, inexpensive and easily available TiO_2 nanoparticles were chosen to construct the rough structures of superhydrophobic materials.

In this study, two different sizes of nano-sized TiO_2 were mixed with chitosan to prepare composite materials with micro-nano level rough structures, and a multifunctional superhydrophobic coating was successfully prepared via low-surface-energy modification with cheap and non-toxic stearic acid.

2 Material and methods

2.1 Material

99.8% metal-based TiO_2 nanoparticles (average particle size of 5–10 nm and 40 nm) were purchased from Shanghai Meryer Chemical Technology Co., Ltd. The chitosan (CS) with deacetylation degree $\geq 95\%$ and viscosity of 100–200 MPa·s was purchased from Shanghai Macklin Biochemical Technology Co., Ltd. Analytical-grade stearic acid ($\text{CH}_3(\text{CH}_2)_{16}\text{COOH}$, SA) was purchased from Tianjin Ruijinte Chemicals Co., Ltd. Furthermore, analytically pure anhydrous ethanol was purchased from the Tianjin Beichen Fangzheng Reagent Factory. Filter paper was provided by the Jiangsu Taizhou Aoke Filter Paper Factory. All chemicals were used as received, and no further purification was required.

2.2 Experimental methods

2.2.1 Surface modification of nanoparticles

First, 0.6 g of stearic acid was added to 30 mL of anhydrous ethanol for ultrasonic dissolution to ensure

that all the stearic acid was evenly dissolved in anhydrous ethanol, and a 20-g/L stearic acid ethanol solution was obtained.

Second, the inexpensive and nontoxic stearic acid was used to modify the nanoparticles. A certain amount of 40 nm-TiO₂ was added to an anhydrous stearic acid ethanol solution, which was vigorously stirred for 1 h at room temperature, and then an ultrasonicated instrument was used for 30 min. To this suspension, 0.12 g of chitosan was added and stirred for 2 h to obtain a TiO₂@SA/CS superhydrophobic coating. Depending on the amount of TiO₂ added, the coatings were named TiO₂@SA/CS-X (X=1, 2, 3, 4, 5; corresponding to additions of 0.6 g, 0.72 g, 0.84 g, 0.96 g, and 1.08 g, respectively). Below, unless otherwise indicated, the TiO₂ additions to the TiO₂@SA/CS coatings in the tests were all 0.84 g. On the basis of the above experiments, in order to investigate the effect of a single component on the interfacial wettability, the TiO₂@SA coating, TiO₂/CS coating, CS@SA coating were prepared by reducing a single component, respectively.

Third, under the premise that the total amount of nano TiO₂ added remains unchanged, two kinds of TiO₂ with different particle sizes (5–10 nm and 40 nm, respectively) were compounded in different ratios, and the coatings were named as TiO₂(A:B)@SA/CS (A : B= 10 : 0, 9 : 1, 7 : 3, 5 : 5, 3 : 7, 1 : 9, 0 : 10) according to the different ratios of the compounding.

2.2.2 Preparation of superhydrophobic paper

The cleaned filter paper was immersed in the superhydrophobic coating prepared above for 10 min, and then the filter paper was slowly removed and placed horizontally in an oven at 80 °C. After drying,

the superhydrophobic paper was finally obtained.

2.3 Measurement and characterization

The surface morphology of the paper before and after the treatment was observed using a field-emission scanning electron microscope (FE-SEM, ZEISS Sigma 500) at 5.0 kV. The surface elemental composition was determined using Fourier-transform infrared spectrometry (FT-IR Spectrometer, PerkinElmer) and X-ray photoelectron spectroscopy (Axis Supra, Shimadzu). An X-ray diffractometer (Ultima IV, Rigaku) was used to analyse the crystal structure of the sample material. An optical contact angle-measuring instrument (JC2000D1, Shanghai Zhongchen Digital Technology Equipment Co., Ltd.) was used to measure the water contact angles (WCA) of the coatings. The static drop method was used to measure the WCA at ambient temperature. A drop of water (approximately 5 μL) is carefully placed on the paper. The average WCA was determined by collecting the same sample from five different locations.

3 Results and discussion

3.1 SEM and wettability

Two key factors in the preparation of superhydrophobic materials are low-surface energy and rough structures. The paper surface morphology was measured via SEM before and after modification, and the influence of the surface morphology on the superhydrophobic properties was discussed.

Fig. 2(a) and Fig. 2(b) show SEM images of the raw paper surface and superhydrophobic paper surface, respectively. It is clear from Fig. 2(a) that the untreated paper mainly comprises reticulated plant fibers with a

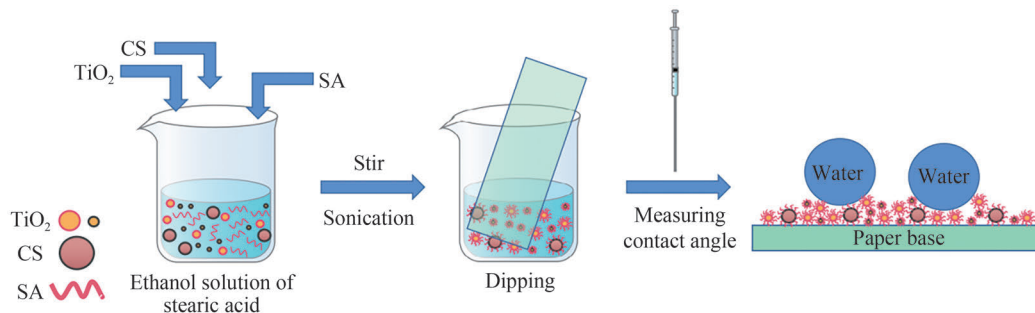


Fig. 1 Schematic diagram of the formation process of superhydrophobic paper

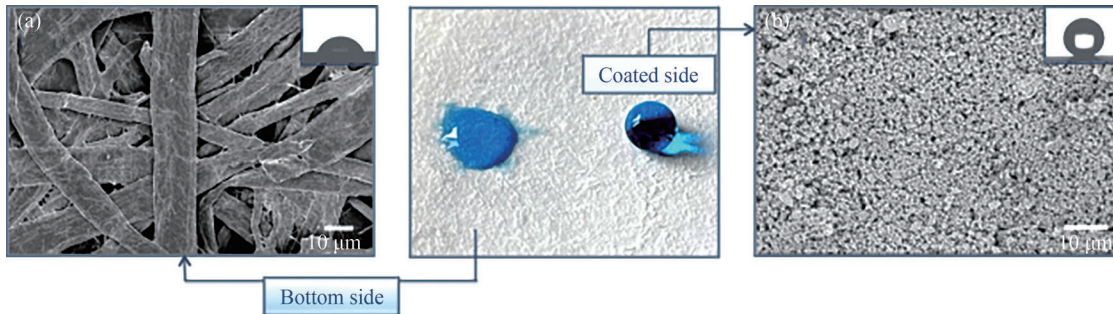


Fig. 2 SEM images of paper with (a) hydrophilic bottom surface and (b) superhydrophobic coated surface

specific rough structure, many gaps, and pores between the fibers. It can be observed from Fig. 2(b) that the microscopic surface morphology of the superhydrophobic paper changes significantly, showing a denser coating when compared to the unmodified paper. Stearic acid-modified TiO_2/CS micro-nano composite particles were deposited on the filter paper surface, filling and completely covering the pores of the original paper. Numerous modified composite particles adhere to the paper surface via physical adsorption. This accumulation, coupled with the irregular positioning of diverse micro-nano particles, creates a multitude of voids and cavities. This results in a paper surface characterized by its micro/nano multi-scale rough texture. Enhancing the paper's surface roughness is crucial for constructing superhydrophobic surfaces.

Wettability was characterized by the contact angle measured on the paper surface. Fig. 3 shows images of

water droplets on the surface of the raw paper, micro-nano composite particles modified paper, stearic acid-reagent-modified paper, and superhydrophobic-coated paper.

Although the paper-based material exhibits a rough surface structure, the paper-based material is hydrophilic prior to modification due to the hydrophilic groups on the surface, and the measured WCA is approximately 70° . When the paper surface is covered with TiO_2/CS micro-nano composite particles, the paper is superhydrophilic and water droplets can be absorbed by the paper instantly because chitosan and nano TiO_2 exhibit strong hydrophilicity, and the micro-nano particles provide high roughness. The measured WCA was approximately 0° . After modification with stearic acid, the surface of the filter paper changed from hydrophilic to hydrophobic, and the WCA changed from 70° to approximately 120° . The sample treated with the $\text{TiO}_2@\text{SA}$ coating exhibited

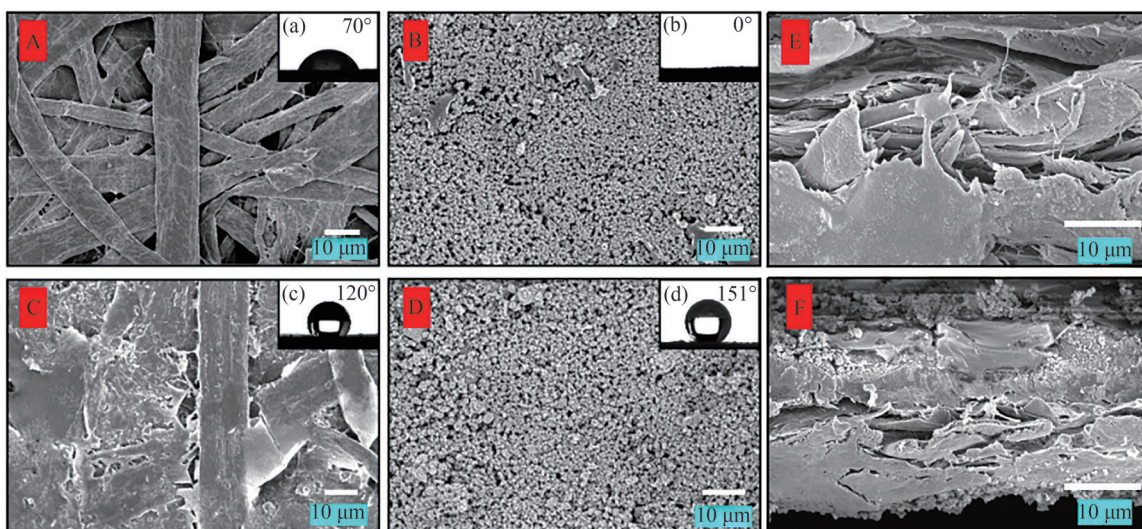


Fig. 3 Images of water droplets on different substrate surfaces: (A) original paper surface; (B) paper surface coated with TiO_2/CS micro-nano composite particles; (C) paper surface modified with stearic acid; (D) paper surface treated with $\text{TiO}_2@\text{SA}/\text{CS}$ coating; (E) and (F) cross-sectional SEM images of original paper and paper treated with $\text{TiO}_2@\text{SA}/\text{CS}$ coating, respectively

high hydrophobicity, and the static contact angle was greater than 140° . Additionally, while it exhibited a significant roll angle—well above 10° —it did not quite achieve the superhydrophobic effect. After depositing TiO_2/CS composite particles followed by a stearic acid treatment, rendering the paper's surface notably hydrophobic, the filter paper's hydrophobicity was further augmented compared with the sample created using $\text{TiO}_2@\text{SA}$. Chitosan contributes to enhancing the composite's resistance to wetting.

While keeping the quantities of immobilized chitosan and stearic acid constant, the impacts of varying TiO_2 amounts on surface wettability by adjusting the quantity of 40-nm TiO_2 were investigated. As depicted in Fig. 4(b), the optimal moisture resistance is observed when the ratio of $\text{TiO}_2 : \text{CS} : \text{SA}$ is $7 : 1 : 5$. The hydrophobic paper exhibited a contact angle of up to 151° and a roll angle of 9° , indicative of its superhydrophobic properties.

It can be observed from Fig. 4(c) that among the

superhydrophobic coatings prepared using composite nanoparticles with different particle sizes, the superhydrophobic coating prepared using composite nano-sized TiO_2 exhibits a better superhydrophobic effect than that prepared using single-sized TiO_2 nanoparticles. When the ratio of 5–10-nm to 40-nm TiO_2 particles was $7 : 3$, it exhibited a contact angle of up to 160° and a roll angle of 3° . Given that the surface roughness is one of the key factors for the formation of superhydrophobic surfaces, AFM was used to further characterize the roughness values of the superhydrophobic coatings, which were $\text{TiO}_2@\text{SA}/\text{CS}$ superhydrophobic coating and $\text{TiO}_2(7 : 3)@\text{SA}/\text{CS}$ superhydrophobic coating. As shown in Fig. 5(a) and Fig. 5(b), it can be demonstrated that the roughness of the paper modified by different superhydrophobic coatings varies significantly, and the superhydrophobic coatings prepared by compounded nanoparticles exhibit better surface roughness. This is due to the fact that a large number of TiO_2 particles, with

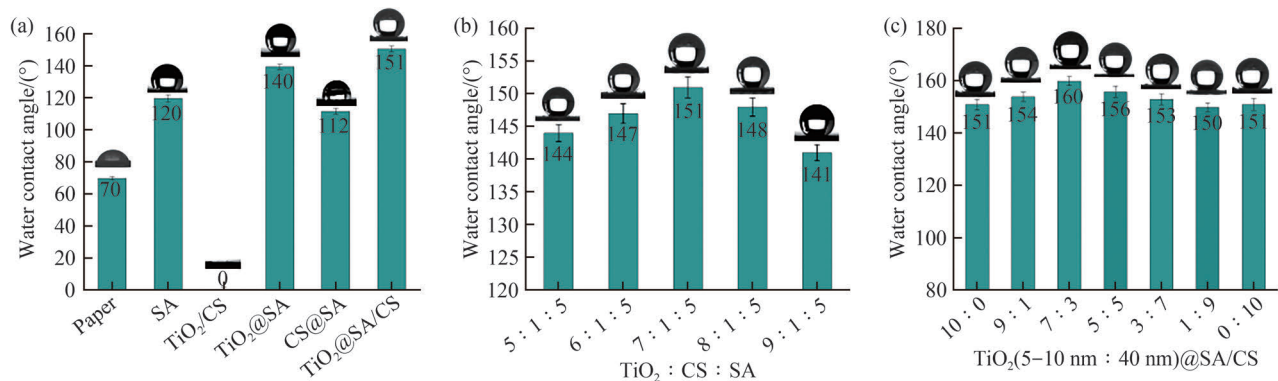


Fig. 4 (a) Effect of superhydrophobic coating components on the WCA of paper surfaces; (b) WCA on the surface of samples prepared with different addition ratios of $\text{TiO}_2 : \text{CS} : \text{SA}$; (c) WCA of $\text{TiO}_2(\text{A} : \text{B})@\text{SA}/\text{CS}$ coatings with different compounding ratios

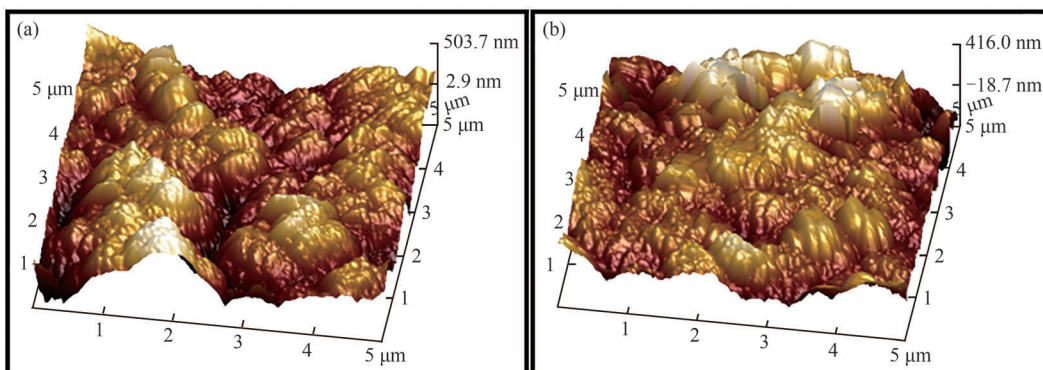


Fig. 5 AFM 3D surface structures of superhydrophobic coatings prepared when the ratio of (a) 5–10-nm to 40-nm TiO_2 particles is $7 : 3$ and (b) superhydrophobic coatings formulated at 40 nm

different particle sizes, gathered together to form a more complex multi-scale hierarchical structure, which resulted in a rougher micro-nano composite structure. According to the Cassie model, liquid droplets do not penetrate rough grooves. Instead, they lie at the solid-air-liquid interface, and the SEM image of the paper cross-section in Fig. 3 also indicates that the superhydrophobic paper surface has a rougher micro-nano-composite structure. When water drops from the coating surface, air is trapped in the micropores and forms an air cushion on the coating surface, forming a liquid-air-solid composite interface, which results in prepared coatings exhibiting superhydrophobicity.

3.2 FT-IR analysis

The presence and binding of stearic acid molecules on the surface of the nanoparticles were investigated via FT-IR. The FT-IR spectra are shown in Fig. 6. The spectra of the stearic acid-modified TiO₂ nanoparticles show peaks at 2914 cm⁻¹ and 2846 cm⁻¹, corresponding to C—H stretching vibrations in methyl (—CH₃) and methylene (—CH₂), respectively. The aforementioned characteristic peaks are all from the nonpolar part of stearic acid, indicating that all the absorption peaks due to the presence of nonpolar part of stearic acid. This indicates that the nano-TiO₂@SA composite-modified superhydrophobic coating had long carbon chains, which were formed by the reaction of nano-TiO₂ with stearic acid.

In the FT-IR spectrum of chitosan, the broad peak at

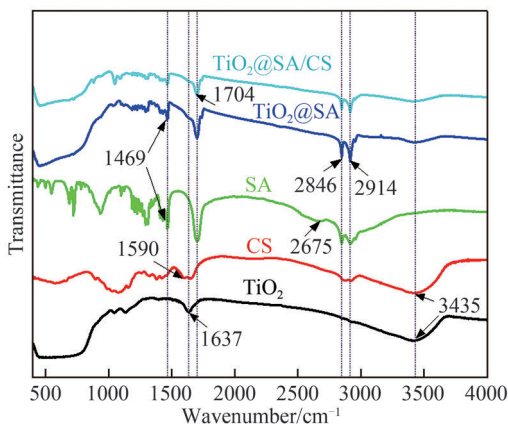


Fig. 6 FT-IR spectra of nano-TiO₂, chitosan, stearic acid, TiO₂@SA, and TiO₂@SA/CS composite particles

approximately 3435 cm⁻¹ corresponds to the stretching vibrations of O—H of the hydroxyl group and N—H of the amino group in chitosan. In the FT-IR spectrum of TiO₂@SA/CS, the broad peak near 3435 cm⁻¹ became obviously smaller, while the absorption peak at 1590 cm⁻¹, belonging to the chitosan amino group, disappeared mainly due to the reaction about —NH₂ of chitosan. Furthermore, stearic acid prevented the formation of hydrogen bonds within and between the chitosan molecules.

Simultaneously, the appearance of absorption peaks at 2914, 2846, and 1704 cm⁻¹ indicated the presence of carboxyl groups in the composites. By comparing the FT-IR spectra of the composites and stearic acid, it was determined that the absorption peaks of the composites became weaker at 1704 cm⁻¹ and 1469 cm⁻¹ and disappeared at 2675 cm⁻¹. Furthermore, the absorption peak of the polar part significantly weakened or disappeared, indicating that only a small amount of stearic acid was absorbed on the surface of the nanoparticles and that there was nearly no free residual fatty acid in the product.

3.3 XPS analysis

TiO₂@SA/CS nanocomposites were successfully positioned on a paper substrate. The uncoated filter paper and superhydrophobic paper coated with the nanocomposite, were analyzed using XPS. In Fig. 7, the uncoated paper shows two different peaks at the binding energies of 283.9 eV and 530.3 eV, corresponding to

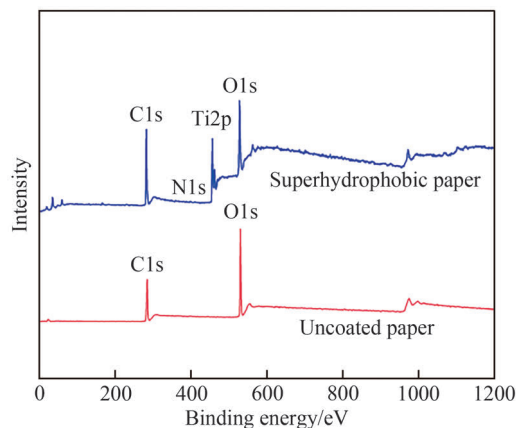


Fig. 7 XPS spectra of uncoated paper surface and superhydrophobic paper surface

carbon atoms (C1s) and oxygen atoms (O1s), respectively. This result was expected because the paper was made of plant fibers basically.

However, despite the presence of oxygen and carbon peaks, the XPS wide-scan spectrum of the superhydrophobic paper exhibited other peaks. The peak with the lowest binding energy (398.9 eV) belongs to the nitrogen atoms (N1s). Among the materials used in this experiment, only chitosan contained N, indicating that it was successfully retained in the superhydrophobic paper. Ti2p peaks representing the TiO₂ nanoparticles were observed at binding energies of 456.2 eV and 461.8 eV. Their intensities were quite high because of the high degree of adsorption of the TiO₂ nanoparticles on the surface layer of the superhydrophobic paper.

Table 1 shows the quantitative atomic contents results based on XPS. With the uncoated paper, 39.25% of the surface layer consisted O1s, and 60.75% of the surface layer consisted C1s. However, for the superhydrophobic paper, the carbon content decreased ([C]=55.14%) because the surface layer adsorbed more TiO₂ nanoparticles on fibers of paper. As shown in Table 1, the C/O ratio of the uncoated paper is 1.55 and that of the prepared superhydrophobic paper increases to 1.72, which increases the proportion of C1s owing to the coating with stearic acid. 12.38% of the superhydrophobic paper surface comprised Ti atom, indicating that TiO₂ nanoparticles were highly adsorbed on the paper surface. The appearance of N1s was attributed to the presence of chitosan macromolecules on the coating surface. A comparison of the full XPS spectra before and after the surface hydrophobic coating treatment showed that the modified paper surface contained Ti and N atoms, indicating that TiO₂ and chitosan were successfully absorbed on the paper surface. The C/O ratio of the coating increased after modification, indicating that the coating surface was successfully modified with stearic acid.

Table 1 Atomic contents for unmodified paper and superhydrophobic paper

Samples	[C]/%	[O]/%	[N]/%	[Ti]/%	C/O
Uncoated paper	60.75	39.25	-	-	1.55
Superhydrophobic paper	55.14	32.01	0.48	12.38	1.72

SEM-EDS was used to investigate the elemental distribution of the TiO₂@SA/CS superhydrophobic paper (Fig. 8). The characteristic elements of the coating include C, O, N, and Ti, and these four elements are evenly distributed in the coating, indicating that the superhydrophobic coating is uniformly modified on the surface of the paper.

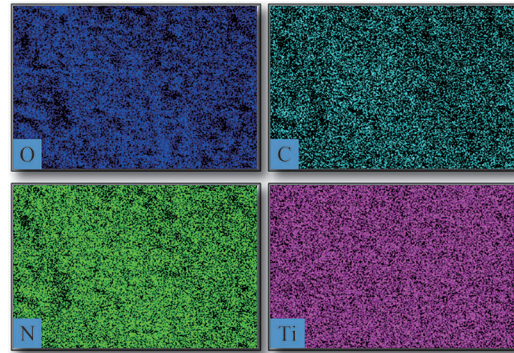


Fig. 8 Elemental mapping of superhydrophobic paper surfaces

3.4 XRD analysis

The XRD patterns of TiO₂ nanoparticles, chitosan, stearic acid, and TiO₂@SA/CS composite coating are shown in Fig. 9. The diffraction pattern of the composite coating was essentially similar to that of TiO₂ nanoparticles, with a particle size of approximately 40 nm. In Fig. 8, the strongest peaks of both the composite coating and TiO₂ nanoparticles are at $2\theta=25.50^\circ$, which represents the (101) crystal plane in TiO₂ crystals, and the other characteristic peaks correspond to the crystal planes labelled in Fig. 9. It is known that the ore type of TiO₂ before and after modification does not change, and it

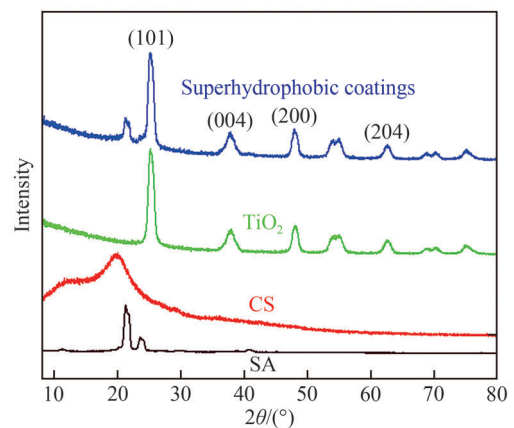


Fig. 9 XRD spectra of nano-TiO₂, chitosan, stearic acid, and TiO₂@SA/CS superhydrophobic coatings

remains consistently as anatase.

Chitosan exhibits two wide characteristic diffraction peaks at $2\theta=11^\circ$ and 20° , and this crystal structure is completely consistent with the reported crystal structure^[41]. The 11° diffraction peak of the superhydrophobic coating disappeared, indicating that the amino group of chitosan reacted with the carboxyl group of stearic acid to form new crystals.

4 Properties of superhydrophobic coated surfaces

4.1 Self-cleaning and liquid-repelling properties

Fig. 10 shows the self-cleaning performance of the $\text{TiO}_2/\text{SA}/\text{CS}$ superhydrophobic composite coating surface. Activated carbon powder was used as a pollutant to characterize the self-cleaning performance of the superhydrophobic composite coating surface. As shown in Fig. 10, the activated carbon powder is sprayed onto the surface of the superhydrophobic composite coating, and then water is dropped onto the surface using a dropper. When the droplet tumbled, the activated carbon powder as pollutant on the coating surface was removed, similar to the dust on the lotus leaf, such that the composite coating surface showed the same excellent self-cleaning performance as the lotus leaf.

As shown in Fig. 10, the prepared superhydrophobic

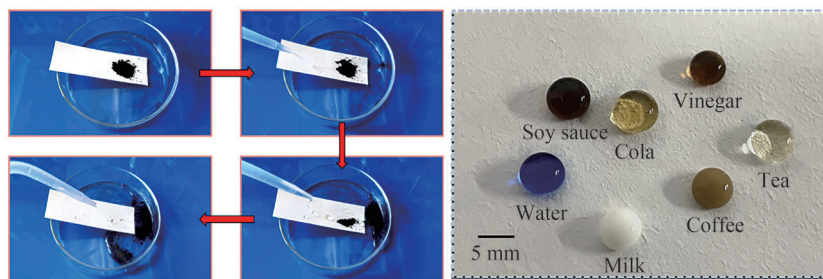


Fig. 10 Self-cleaning performance test and rejection test of the prepared superhydrophobic paper with respect to various liquids

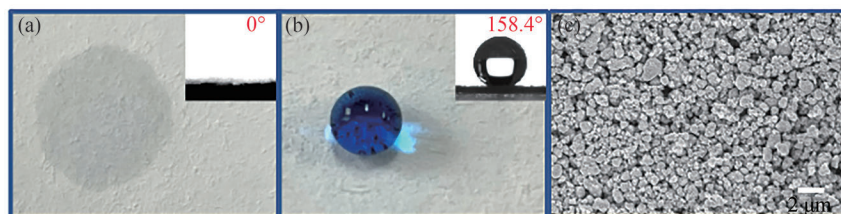


Fig. 11 Antifouling properties test of superhydrophobic paper: (a) diffusion of the ethanol droplet ($5\ \mu\text{L}$) on the coating surface; (b) the water droplet on the coating surface after evaporation of ethanol; (c) SEM image of paper surface after evaporation of ethanol

surfaces exhibited good liquid repellency to various common liquids, such as coffee, milk, soy sauce, vinegar, tea, and cola. The contact angles of various droplets were greater than 150° . The pores of the prepared superhydrophobic surfaces capture a large layer of air, which effectively prevents the penetration of liquid droplets.

4.2 Antifouling properties and chemical stability resistance

Furthermore, the coating exhibited good antifouling properties in organic solvents with low boiling points such as toluene, chloroform, ethanol, and acetone. When an organic solvent was dropped onto the coating surface, the surface was instantly wetted, and the contact angle was approximately 0° . However, after approximately 50 s under natural conditions, the organic layer completely evaporated, and the surface regained its superhydrophobic behavior (Fig. 11(b)). SEM characterization of the samples after the evaporation of the low-boiling-point solvent was performed. The results are shown in Fig. 11(c) wherein a rough micro/nano structure still exists on the paper surface, which proves that the microstructure of the coating has not been destroyed by low-boiling-point solvent. Therefore, the coating exhibits good antifouling performance against organic solvents to some extent.

The prepared $\text{TiO}_2(7 : 3)/\text{SA}/\text{CS}$ superhydrophobic

coating surface showed excellent chemical resistance to acids with different pH values, alkalis with lower pH values, and 3.5-wt% NaCl solution. It can be observed from Fig. 12 that the contact angle of solutions with pH values from 2 to 10 varied from 154° to 158° , indicating that the prepared superhydrophobic surface has superior acid resistance while weak alkaline resistance. When a strong alkaline solution with a pH value of 13 was dropped onto the superhydrophobic coating surface, the surface lost its superhydrophobicity. This is due to the fact that when the coating encounters a strong alkaline solution it produces stearate, which destroys the chemical composition of the coating surface and changes the surface from superhydrophobic to superhydrophilic with an approximate contact angle of 0° . The results showed that the prepared superhydrophobic coating surface exhibits good chemical stability for solution with specific pH value and antifouling properties in some organic solvents.

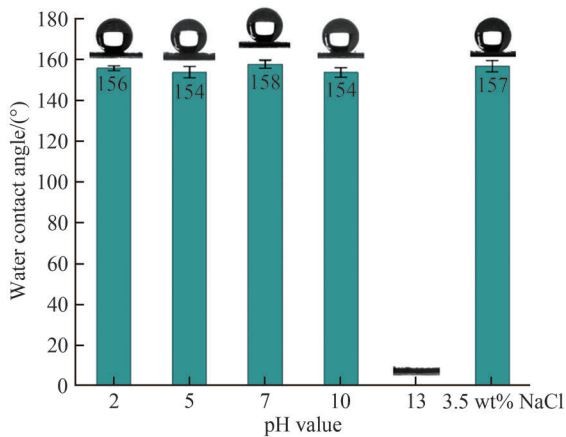


Fig. 12 WCA of the $\text{TiO}_2(7:3)@SA/CS$ superhydrophobic paper for solutions with different pH values

4.3 Repairability

In practical applications, superhydrophobic coating surfaces are prone to mechanical wear, which makes them easily lose their superhydrophobicity. The use of easily repairable coating surfaces is an effective method for increasing wear resistance and alleviating the problem of mechanical damage. The coating prepared in this study is also susceptible to mechanical scratching (Fig. 13(a)) because a strong chemical bond between the coating and paper substrate does not exist. However, given that the manufacturing method is simple and time

saving, it provides an opportunity to build a regenerative system. When the mechanically damaged paper was dipped into the superhydrophobic coating and air-dried, the damaged paper surface exhibited superhydrophobicity (Fig. 13(b)). Hence, the ability for easy repair is anticipated to satisfy the requirements for superhydrophobicity in future practical applications.

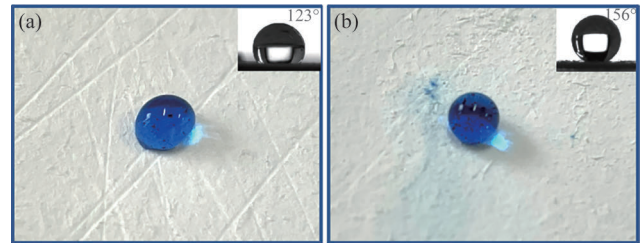


Fig. 13 Photographs of water droplets on (a) a damaged paper surface and (b) a regenerated superhydrophobic surface

5 Conclusion

Multifunctional superhydrophobic coating surfaces on paper substrates were successfully prepared using a simple and efficient solution impregnation method in this study. The advantage of this preparation method is that the raw materials are inexpensive and fluorine-free. It does not rely on expensive or fluorine-containing chemicals to generate a superhydrophobic surface, and the preparation process was simple which only uses ethanol as a dispersant.

The optimal moisture resistance is observed when the ratio of $\text{TiO}_2 : \text{CS} : \text{SA}$ is $7 : 1 : 5$, the hydrophobic paper exhibited a contact angle of up to 151° and a roll angle of 9° , indicative of its superhydrophobic properties. Additionally, the coatings prepared by compounding TiO_2 with different nanoparticle sizes exhibited superior superhydrophobicity under the same conditions, indicating that the compounding of nanoparticles can provide a rough micro-nano structure, which is more conducive to superhydrophobic properties.

The prepared superhydrophobic paper exhibited good self-cleaning properties, organic solvent antifouling properties, liquid repellency, and chemical stability. Although the prepared coatings can be easily scratched mechanically, owing to their simple preparation method, superhydrophobic coatings are easy to repair via

re-immersion and exhibit wide potential for practical applications.

Acknowledgments

The authors are grateful for the financial support from the Key Research and Development Project of Shandong Province (2019GHY112040), National Natural Science Foundation of China (22078167), Youth Innovative Team Development Plan of Colleges and Universities in Shandong Province (2019KJC008), Shandong Province Major Innovation Project (2018CXGC1001), and Foundation (No. XWZR201901) of the State Key Laboratory of Bio-based Material and Green Papermaking, Qilu University of Technology; and Major Innovation Project of Qingdao West Coast (2019-27). Shandong Province Key Supporting Areas for Introducing Urgently Needed and Shortage of Talents Project - Key Technology Research and Development and Industrialization of Highly Water-Resistant Biomass-Based Materials.

Conflicts of interest

The authors declare no conflict of interest. The authors declare that they have no competing financial interests or personal relationships that may have influenced the research reported in this study.

References

- [1] ZHANG L, WU J, HEDHILI M N, YANG X, WANG P. Inkjet printing for direct micropatterning of a superhydrophobic surface: toward biomimetic fog harvesting surfaces. *Journal of Materials Chemistry A*, 2015, 3 (6), 2844-2852.
- [2] SIMPSON J T, HUNTER S R, AYTUG T. Superhydrophobic materials and coatings: a review. *Reports on Progress in Physics*, 2015, DOI: 10.1088/0034-4885/78/8/086501.
- [3] LIU Y, BAI Y, JIN J, TIAN L, HAN Z, REN L. Facile fabrication of biomimetic superhydrophobic surface with anti-frosting on stainless steel substrate. *Applied Surface Science*, 2015, 355, 1238-1244.
- [4] LATTHE S S, SUTAR R S, KODAG V S, BHOSALE A K, KUMAR A M, SADASIVUNI K K, XING R M, LIU S H. Self-cleaning superhydrophobic coatings: Potential industrial applications. *Progress in Organic Coatings*, 2019, 128, 52-58.
- [5] BHUSHAN B, JUNG Y C. Natural and biomimetic artificial surfaces for superhydrophobicity, self-cleaning, low adhesion, and drag reduction. *Progress in Materials Science*, 2011, 56 (1), 1-108.
- [6] YANG J, LONG F, WANG R, ZHANG X, YANG Y, HU W, LIU L. Design of mechanical robust superhydrophobic Cu coatings with excellent corrosion resistance and self-cleaning performance inspired by lotus leaf. *Colloids and Surfaces A-Physicochemical and Engineering Aspects*, 2021, DOI: 10.1016/j.colsurfa.2021.127154.
- [7] NEINHUIS W B J P. Purity of the sacred lotus, or escape from contamination in biological surfaces. *Planta*, 1997, 202 (1), 1-8.
- [8] FENG L, ZHANG Y, XI J, ZHU Y, WANG N, XIA F, JIANG L. Petal effect: A superhydrophobic state with high adhesive force. *Langmuir*, 2008, 24 (8), 4114-4119.
- [9] LI A, WANG G, ZHANG Y, ZHANG J, HE W, REN S, XU Z, WANG J, MA Y. Preparation methods and research progress of superhydrophobic paper. *Coordination Chemistry Reviews*, 2021, DOI: 10.1016/j.ccr.2021.214207.
- [10] CHEN H, WANG B, LI J, YING G, CHEN K. High-strength and super-hydrophobic multilayered paper based on nano-silica coating and micro-fibrillated cellulose. *Carbohydrate Polymers*, 2022, DOI: 10.1016/j.carbpol.2022.119371.
- [11] RAMESH M, PALANIKUMAR K, REDDY K H. Plant fibre based bio-composites: Sustainable and renewable green materials. *Renewable & Sustainable Energy Reviews*, 2017, 79, 558-584.
- [12] SAMYN P. Wetting and hydrophobic modification of cellulose surfaces for paper applications. *Journal of Materials Science*, 2013, 48 (19), 6455-6498.
- [13] WEN Q, GUO F, YANG F, GUO Z. Green fabrication of coloured superhydrophobic paper from native cotton cellulose. *Journal of Colloid and Interface Science*, 2017, 497, 284-289.
- [14] ZHANG W, LU P, QIAN L, XIAO H. Fabrication of superhydrophobic paper surface via wax mixture coating. *Chemical Engineering Journal*, 2014, 250, 431-436.
- [15] XUE C, FAN Q, GUO X, AN Q, JIA S. Fabrication of superhydrophobic cotton fabrics by grafting of POSS-based polymers on fibers. *Applied Surface Science*, 2019, 465, 241-248.
- [16] HOU K, ZENG Y, ZHOU C, CHEN J, WEN X, XU S, CHENG J, PI P. Facile generation of robust POSS-based superhydrophobic fabrics via thiol-ene click chemistry. *Chemical Engineering Journal*, 2018, 332, 150-159.
- [17] PENG L, MENG Y, LI H. Facile fabrication of superhydrophobic paper with improved physical strength by a novel layer-by-layer assembly of polyelectrolytes and lignosulfonates-amine. *Cellulose*, 2016, 23 (3), 2073-2085.
- [18] WANG Y, PENG H, LI T, SHIU B, ZHANG X, LOU C, LIN J. Lightweight, flexible and superhydrophobic conductive composite films based on layer-by-layer self-assembly for high-performance electromagnetic interference shielding. *Composites Part A-Applied Science and Manufacturing*, 2021, DOI: 10.1016/j.compositesa.2020.106199.
- [19] OZBAY S, CENGIZ U, ERBIL H Y. Solvent-Free

- Synthesis of a Superamphiphobic Surface by Green Chemistry. *ACS Applied Polymer Materials*, 2019, 1 (8), 2033-2043.
- [20] DIMITRAKELLIS P, TRAVLOS A, PSYCHARIS V P, GOGOLIDES E. Superhydrophobic Paper by Facile and Fast Atmospheric Pressure Plasma Etching. *Plasma Processes and Polymers*, 2017, DOI: 10.1002/ppap.201600069.
- [21] KIM D, HAN J, MAUCHAUFFE R, KIM J, MOON S Y. Antithetic superhydrophobic/superhydrophilic surfaces formation by simple gas switching in an atmospheric-pressure cold plasma treatment. *Materials Chemistry and Physics*, 2022, DOI: 10.1016/j.matchemphys.2021.125482.
- [22] SEYFI J, PANAHI-SARMAD M, ORAIEGHODOUSI A, GOODARZI V, KHONAKDAR H A, ASEFNEJAD A, SHOJAEI S. Antibacterial superhydrophobic polyvinyl chloride surfaces via the improved phase separation process using silver phosphate nanoparticles. *Colloids and Surfaces B-Biointerfaces*, 2019, DOI: 10.1016/j.colsurfb.2019.110438.
- [23] LIU Z, REN L, JING J, WANG C, LIU F, YUAN R, JIANG M, WANG H. Fabrication of robust superhydrophobic organic-inorganic hybrid coating through a novel two-step phase separation method. *Progress in Organic Coatings*, 2021, DOI: 10.1016/j.porgcoat.2021.106320.
- [24] SUN H, LIU Z, LIU K, GIBRIL M E, KONG F, WANG S. Lignin-based superhydrophobic melamine resin sponges and their application in oil/water separation. *Industrial Crops and Products*, 2021, DOI: 10.1016/j.indcrop.2021.113798.
- [25] CHEN C, LI C, YU D, WU M. A facile method to prepare superhydrophobic nanocellulose- based aerogel with high thermal insulation performance via a two-step impregnation process. *Cellulose*, 2022, 29 (1), 245-257.
- [26] RAMAN A, JAYAN J S, DEERAJ B D S, SARITHA A, JOSEPH K. Electrospun Nanofibers as Effective Superhydrophobic Surfaces: A Brief review. *Surfaces and Interfaces*, 2021, DOI: 10.1016/j.surfin.2021.101140.
- [27] ZHANG M, YANG Q, GAO M, ZHOU N, SHI J, JIANG W. Fabrication of Janus cellulose nanocomposite membrane for various water/oil separation and selective one-way transmission. *Journal of Environmental Chemical Engineering*, 2021, DOI: 10.1016/j.jece.2021.106016.
- [28] MOSAYEBI E, AZIZIAN S, NOEI N. Preparation of Robust Superhydrophobic Sand by Chemical Vapor Deposition of Polydimethylsiloxane for Oil/Water Separation. *Macromolecular Materials and Engineering*, 2020, DOI: 10.1002/mame.202000425.
- [29] ZHANG S, LI W, WANG W, WANG S, QIN C. Reactive superhydrophobic paper from one-step spray-coating of cellulose-based derivative. *Applied Surface Science*, 2019, DOI: 10.1016/j.apsusc.2019.143816.
- [30] XUE F, SHI X, BAI W, LI J, LI Y, ZHU S, LIU Y, FENG L. Enhanced durability and versatile superhydrophobic coatings via facile one-step spraying technique. *Colloids and Surfaces A-Physicochemical and Engineering Aspects*, 2022, DOI: 10.1016/j.colsurfa.2022.128411.
- [31] ZHANG J, CHEN R, LIU J, LIU Q, YU J, ZHANG H, JING X, LIU P, WANG J. Superhydrophobic nanoporous polymer-modified sponge for in situ oil/water separation. *Chemosphere*, 2020, DOI: 10.1016/j.chemosphere.2019.124793.
- [32] RAEISI M, KAZEROUNI Y, MOHAMMADI A, HASHEMI M, HEJAZI I, SEYFI J, KHONAKDAR H A, DAVACHI S M. Superhydrophobic cotton fabrics coated by chitosan and titanium dioxide nanoparticles with enhanced antibacterial and UV-protecting properties. *International Journal of Biological Macromolecules*, 2021, 171, 158-165.
- [33] AKTAS O C, SCHRODER S, VEZIROGLU S, GHORI M Z, HAIDAR A, POLONSKYI O, STRUNSKUS T, GLEASON K, FAUPEL F. Superhydrophobic 3D Porous PTFE/TiO₂ Hybrid Structures. *Advanced Materials Interfaces*, 2019, DOI: 10.1002/admi.201801967.
- [34] ELZAABALAWY A, VERBERNE P, MEGUID S A. Multifunctional Silica-Silicone Nanocomposite with Regenerative Superhydrophobic Capabilities. *ACS Applied Materials & Interfaces*, 2019, 11 (45), 42827-42837.
- [35] LI X, ZHAO S, HU W, ZHANG X, PEI L, WANG Z. Robust superhydrophobic surface with excellent adhesive properties based on benzoxazine/epoxy/mesoporous SiO₂. *Applied Surface Science*, 2019, 481, 374-378.
- [36] YANG C, CUI S, WENG Y, WU Z, LIU L, MA Z, TIAN X, FU R K, CHU P K, WU Z. Scalable superhydrophobic T-shape micro/nano structured inorganic alumina coatings. *Chemical Engineering Journal*, 2021, DOI: 10.1016/j.cej.2020.128142.
- [37] ZHANG B, XU W, ZHU Q, HOU B. Scalable, fluorine free and hot water repelling superhydrophobic and superoleophobic coating based on functionalized Al₂O₃ nanoparticles. *Journal of Materials Science & Technology*, 2021, 66, 74-81.
- [38] WANG Y, CHEN X, LIANG Y, YU C. Fabrication of Super-hydrophobic Filter Paper via Mixed Wax Phase Separation for Efficient Oil/Water Separation. *Bioresources*, 2021, 16 (3), 5794-5805.
- [39] RAGHU S N V, CHULUUNBANDI K, KILLIAN M S. Zirconia nanotube coatings - UV-resistant superhydrophobic surfaces. *Surfaces and Interfaces*, 2021, DOI: 10.1016/j.surfin.2021.101357.
- [40] BHARATHIDASAN T, SATHIYANARYANAN S. Self-replenishing superhydrophobic durable polymeric nanocomposite coatings for heat exchanger channels in thermal management applications. *Progress in Organic Coatings*, 2020, DOI: 10.1016/j.porgcoat.2020.105828.
- [41] KWEON H, UM I C, PARK Y H. Structural and thermal characteristics of *Antheraea pernyi* silk fibroin/chitosan blend film. *Polymer*, 2001, 42 (15), 6651-6656. [PBM](#)